ECS Transactions, 85 (8) 213-218 (2018)
10.1149/08508.0213ecst ©The Electrochemical Society

Ultra-Fast Switching of a Free Magnetic Layer with Out-of-Plane Magnetization in Spin-Orbit Torque MRAM Cells

A. Makarov, V. Sverdlov, and S. Selberherr

Institute for Microelectronics, TU Wien, Wien 1040, Austria

The steady increase in performance and speed of modern integrated circuits is continuously supported by constant miniaturization of complementary metal-oxide semiconductor devices. However, the rapid growth of the dynamic and stand-by power due to transistor leakages becomes a pressing issue. A promising way to interrupt this trend is to introduce non-volatility. The development of an electrically addressable non-volatile memory combining high speed and high endurance is essential for achieving these goals. The perpendicular spin-orbit torque magnetic random access memory (SOT-MRAM) combines non-volatility, high speed, and high endurance and is thus suitable for applications in caches. However, its development is still hindered by the necessity of a static in-plane magnetic field. We propose a magnetic field-free perpendicular SOT-MRAM, operated by two consecutive perpendicular current pulses, which is fast and, most importantly, does not require an external magnetic field.

Introduction

Spin-transfer torque magnetoresistive RAM (STT-MRAM) is fast (10ns), possesses high endurance (10^{12}), and a simple structure. It is compatible with complementary metal-oxide semiconductor devices (CMOS) and can be straightforwardly embedded in circuits (1). High-density STT-MRAM arrays with 4Gbit capacities have been already demonstrated (2). Although the use of STT-MRAM in last-level caches is conceivable (3), the switching current for operating STT-MRAM at faster than 10ns speed is rapidly growing. The development of an electrically addressable non-volatile memory combining high speed (sub-ns operation) and high endurance is essential for replacing SRAM in higher-level caches.

Among the newly discovered physical phenomena suitable for using in next-generation MRAM is the spin-orbit torque (SOT) assisted switching at room temperature in heavy metal/ferromagnetic (4,5) or topological insulator(TI)/ferromagnetic (6,7) bilayers. By passing the current through the heavy material or the TI, the SOT is generated, which acts on the free layer. In this case the large switching current is injected in-plane along the heavy metal/ferromagnetic bilayer and does not flow through the magnetic tunnel junction. This results in a three-terminal configuration (8), in which the read and write current paths are decoupled.

However, SOTs acting on a free ferromagnetic layer do not guarantee deterministic magnetization switching. In particular, to reverse the magnetization of a free layer with a perpendicular magnetic anisotropy (9), an external magnetic field is required (10). The role of this external magnetic field is to break the mirror symmetry of the structure with respect to the plane formed by the easy magnetization orientation and the in-plane current

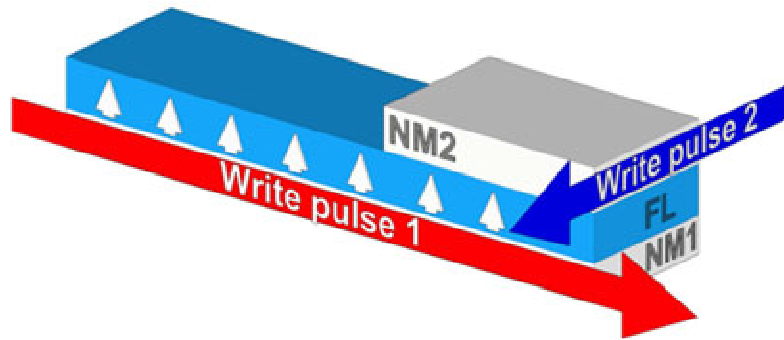

Figure 1. Perpendicular SOT-MRAM memory cell with a 52.5nm × 12.5nm × 2nm free layer. Two consecutive current pulses are applied. The duration of the first pulse is fixed at 100ps. The current amplitude of both pulses is 100μA.

direction. The magnetic field reduces the thermal stability of MRAM cells and complicates the MRAM integration. Several strategies were recently pursued to break this mirror symmetry and to achieve deterministic switching without an external magnetic field: to grow the ferromagnetic layer in a special wedge form (11), to control the spin-orbit torque through crystal symmetry in WTe_2/ferromagnet bilayers (5), to use an antiferromagnetic (AF) material to magnetically bias the ferromagnetic layer (12-15), and to exploit the geometry of the device shape to control the switching (16). However, these methods either require a local intrusion into the fabrication process, or are based on solutions whose scalability and integration is problematic (AF, shapes). Therefore, the development of alternative magnetic field-free SOT-based switching schemes is paramount.

Two-pulse Switching Scheme

Recently we have shown that a switching scheme employing two perpendicular consecutive current pulses is efficient for switching of an in-plane structure (17). Here we demonstrate that the two-pulse scheme is also suitable for fast sub-0.5ns SOT assisted switching of perpendicular structures. Figure 1 schematically illustrates the proposed switching scheme of a free magnetic layer in a SOT-MRAM cell. The first pulse tilts the magnetization away from its equilibrium position and brings it in-plane perpendicular to the “Write pulse 1” current flow. The first pulse, however, cannot reliably switch the magnetization as it does not provide the torque to drag the magnetization from the in-plane orientation to either up or down position. The magnetization recovers its equilibrium perpendicular orientation after the torque is turned off; however, the exact direction – up or down – is random as it is determined by random thermal magnetization fluctuations. If the external in-plane magnetic field parallel to the current direction were applied, it would result in the magnetization precession and move the magnetization deterministically away from the in-plane orientation thus completing the switching.

Here instead of the magnetic field we employ a second perpendicular pulse to achieve deterministic switching. It is important that the second pulse does not run under the whole free layer but through a part of it. It breaks the mirror symmetry and makes the switching deterministic. Below we describe the simulation methodology and the main results.

Simulation Method

The magnetization dynamics of the magnetic system due to spin current densities and spin accumulations is well described by the Landau-Lifshitz-Gilbert equation (18):

$$\frac{\partial \mathbf{m}}{\partial t} = -\gamma \mathbf{m} \times \mathbf{H}_{\text{eff}} + \boldsymbol{\alpha} \mathbf{m} \times \frac{\partial \mathbf{m}}{\partial t} + \gamma \frac{\hbar}{2e} \frac{\Theta_{SH} J}{M_0 d} \mathbf{m} \times (\mathbf{m} \times \mathbf{y}) \quad [1]$$

m is the position-dependent magnetization **M** normalized by the saturation magnetization M_0: **m**= **M**/M_0, γ is the gyromagnetic ratio, α is the Gilbert damping parameter, *e* is the electron charge, ħ is the reduced Plank constant, and Θ_{SH} is an effective Hall angle relating the strength of the spin current density to the charge current density *J*. If the charge current flows along direction **x** in the heavy metal line, the spin current floats perpendicularly along the **z** direction from the heavy metal to the free ferromagnetic layer of thickness *d*. The polarization of the spin current is pointing out along direction $\boldsymbol{y}$ perpendicular to both the spin and charge current directions. The spin polarization entering into the free ferromagnetic layer is becoming quickly aligned with the local magnetization **M** generating the torque (19) acting on the magnetization as described by the last term in [1]. This spin-orbit torque together with the magnetic field $\mathbf{H}_{\text{eff}}$ describes the damped magnetization dynamics [1]. The magnetic field $\mathbf{H}_{\text{eff}}$ includes the external field as well as the contributions due to both bulk and interface-induced magnetic anisotropies, exchange field, and demagnetization field. Thermal effects on the magnetization dynamics are incorporated by means of the random magnetic field added to $\mathbf{H}_{\text{eff}}$. The strength of the thermal field fluctuations is proportional to temperature (20).

We are using the two-pulse switching scheme previously proposed for efficient switching of an in-plane structure (17). The SOT due to the first 100ps pulse through the nonmagnetic heavy metal line NM1 tilts the magnetization of the free layer in-plane perpendicular to the direction of the "Write pulse 1" (Figure 1). The SOT of the second consecutive pulse results in an additional precession of the magnetization in the part of the free layer under the second wire NM2. The current values of both pulses are fixed at 100μA. For the heavy metal wires of dimension 3nm thickness × 12.5nm width, it results in a current density 2.6×10^{12} A/m^2 which is only slightly above the critical current density 2×10^{12} A/m^2 measured in similar structures (10). The additional parameters used in the simulations are summarized in Table 1.

Table 1. Parameters used in the simulations.

Name	Symbol	Value
Saturation magnetization	M_0	4×10^5 A/m.
Exchange constant	A	1×10^{-11} J/m.
Perpendicular anisotropy	K	2×10^5 J/m^3

Results

We performed extensive simulations of the free layer switching for several durations of the second pulse as a function of the width of the second pulse wire. The duration of the first pulse, which must bring the magnetization in- plane perpendicular to the first pulse current, is fixed at 0.1ns. The current density is higher than the critical switching density (10). Figure 2 displays typical dependences of the magnetization dynamics m_z projected on the perpendicular axis OZ, for the MM2 wire widths equal to 5nm, 15nm, and 25nm, correspondingly. We note that, because the current in the pulses is fixed to 100µA, the current densities in Figure 2 are not equal as they scale inversely proportional to the NM2 width.

Due to the "Write pulse 1" the magnetization rapidly comes in-plane in Figure 2 with m_z=0. The second pulse running in the perpendicular direction (Figure 1) rotates the magnetization in-plane under the NM2 wire perpendicular to the "Write pulse 2" current flow. This rotation is transferred to the remaining part of the free layer through the exchange interaction. Depending on the direction of the precession, the magnetization of the remaining part tilts up or down with respect to the in-plane orientation. The part under the wire of "Write pulse 2" follows the precession after the current is turned off, thus completing the switching.

Figure 2a shows the dependence of the switching on the duration of "Write pulse 2". Each curve is the result of averaging over 20 different switching processes with different initial microscopic magnetization realizations obtained after 100ps of thermalization processes in the corresponding random magnetic field (20). The switching is completed even when the second pulse is only 50ps long, with the total switching time gradually increasing for longer pulse durations of "Write pulse 2". The switching time is determined by the condition when the magnetization projection reaches the value m_z=-0.5 is estimated as 500ps for a "Write pulse 2" of 50ps. Another important characteristic of the switching process is the relaxation time which is required for the magnetization to decay to m_z=-0.9 beginning with m_z=-0.5. We note that, although the switching is fast, the current density is unreasonably high and may exceed the electromigration limit as the fixed current of 100µA runs through a very narrow, only 5nm wide, NM2 wire.

Figure 2b demonstrates the time dependence of the magnetization m_z in the case when the second current pulse runs through the NM2 wire of 15nm. In this case the current densities through NM1 and NM2 are almost equal. The switching appears to be also very similar for different pulse durations of "Write pulse 2". We first note that the switching is accelerated to become shorter as 300ps. Second, the switching becomes independent of the pulse durations. Third, the spin relaxation time needed to reach m_z = -0.9 from m_z=-0.5 is also very similar for all pulse durations. It implies that the practical constraints on the pulse duration and synchronization are not restrictive for 15nm width of the NM2 wire, which makes the two-pulse switching scheme attractive for practical realization of perpendicular structure magnetization reversal.

Figure 2c shows the time dependence of the magnetization m_z for 25nm width of the NM2 wire. It takes longer to switch the magnetization from m_z=1 to m_z=-0.5 for shorter "Write pulse 2". A similar time is required for the magnetization to relax independently of the "Write pulse 2" duration.

Finally, if one increases the width of NM2 to 52.5nm thus achieving a complete overlap, the second current pulse leaves the magnetization in-plane and only rotates it perpendicular to the "Write pulse 2" current direction. In this case no deterministic

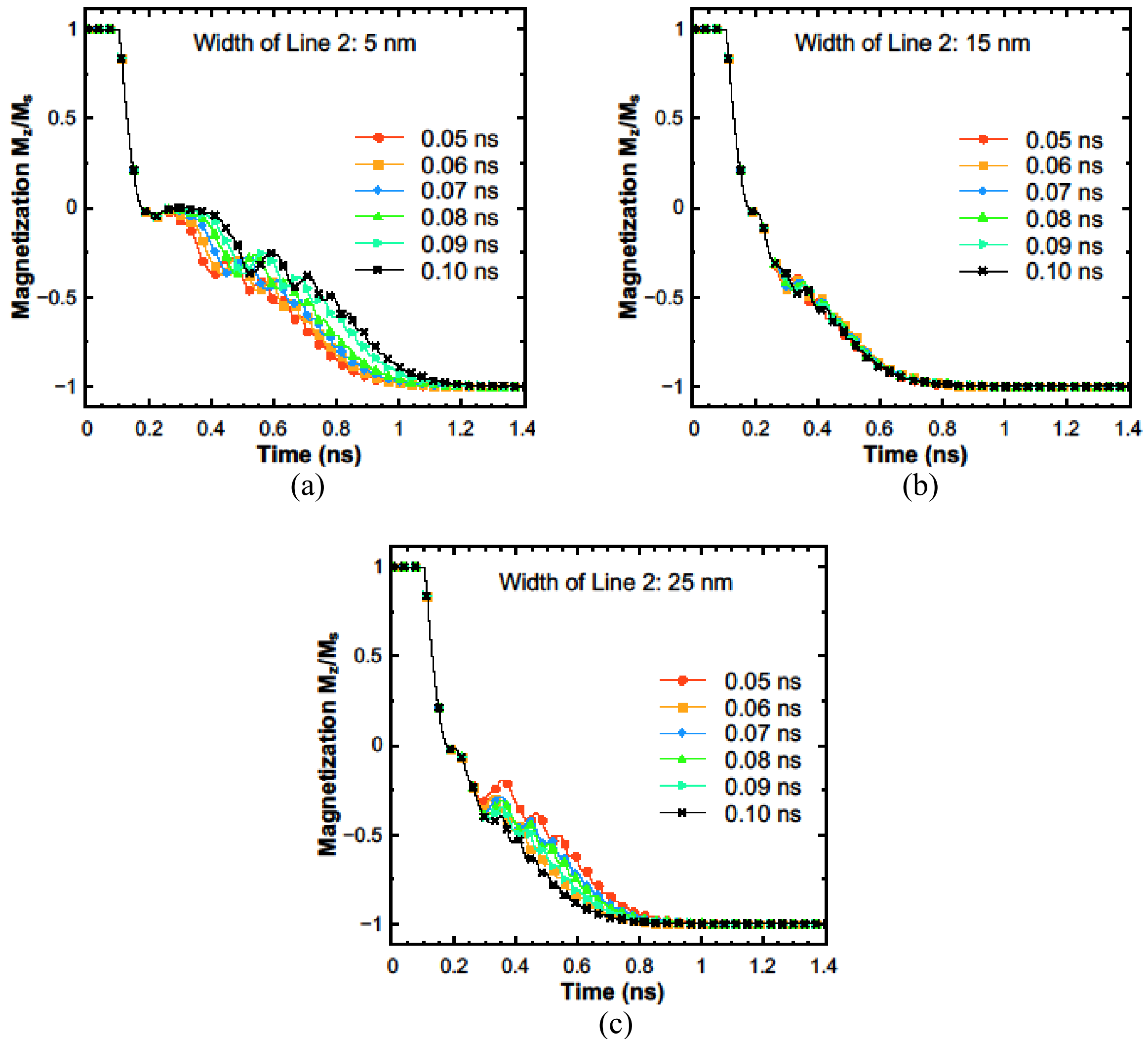

Figure 2. Magnetization switching dynamics as a function of time, for several durations of the second current pulse T_2. The first pulse is fixed at 100ps. The width of the NM2 wire for the second pulse is: 5nm (a), 15nm (b), 25nm (c) (see Figure 1).

switching is achieved. Therefore, the key for the deterministic switching in the two-pulse scheme is the finite overlap of the NM2 wire with the free layer.

Figure 3 displays the dependence of the switching time on the width of the NM2 wire, for several durations T_2 of the second pulse. We conclude that the fastest, sub-300ps switching, is achieved when the overlap is at around 30%.

Conclusion

The two-pulses scheme is shown to be efficient and fast (sub 0.3ns) for SOT-assisted switching of a free magnetic layer with perpendicular magnetic anisotropy. The switching does not require an external magnetic field. It is demonstrated that the fastest switching appears, when the width of the second current carrying wire is about one third of the free layer width. Importantly, requirements to the pulse duration and synchronization are also relaxed, when the width of the second wire is around 30% of the free layer width.

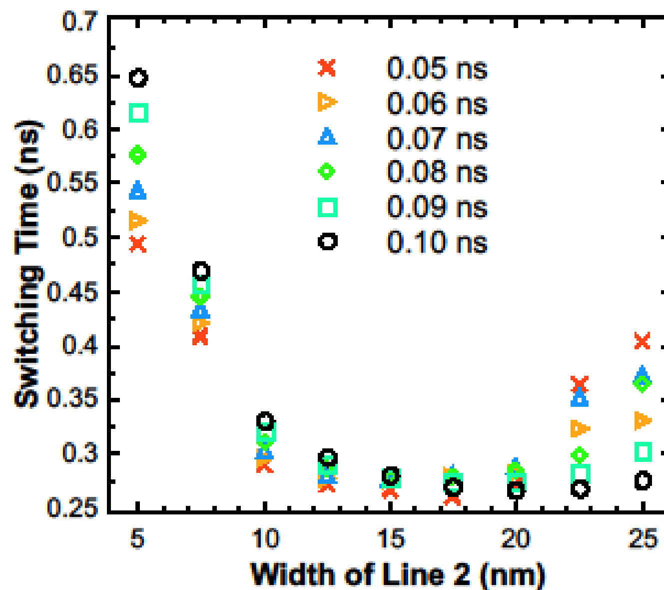

Figure 3. Switching time as a function of the second line width, for several durations of the second pulse, $I_1=I_2=100\mu A$. The temperature is 300K. Each point is a result of averaging over 20 realizations.

References

1. D. Apalkov, B. Dieny, and J.M. Slaughter, *Proceedings of the IEEE* **104**, 1796 (2016).
2. S.-W. Chung, T. Kishi, J. W. Park *et al.*, in *IEDM 2016 Techn. Digest*, p.660 (2016).
3. G.Jan, L.Thomas, S.Le, *et al.*, in *Symp. VLSI Technology*, p.18 (2016).
4. I.M.Miron, G.Gaudin, S.Auffret *et al.*, *Nature Materials* **9**, 230 (2010).
5. D.MacNeil, G.M.Stiehl, M.H.D.Guimaraes *et al.*, *Nature. Physics* **13**, 300 (2017).
6. J.Han, A.Richardella, S.A.Siddiqui *et al.*, *Phys.Rev.Lett*. **119**, 077702 (2017).
7. Y.Wang, D.Zhu, Y.Wu *et al.*, *Nature Communications* **8**, 1364 (2017).
8. S.-W. Lee and K.-J. Lee, *Proceedings of the IEEE* **104**, 1831 (2016).
9. K.Garello, C.O.Avci, I.M.Miron *et al.*, *Appl.Phys.Lett*. **105**, 212402 (2014).
10. S.Fukami, T.Anekawa, C.Zhan, and H.Ohno, *Nature Nanotechnology* **11**, 621 (2016).
11. G.Yu, P.Upadhyaya, Y.Fan, *et al.*, *Nature Nanotechnology* **9**, 548 (2014).
12. S.Fukami, C.Zhang, S.DuttaGupta *et al.*, *Nature Materials* **15**, 535 (2016).
13. A. van den Brink, G.Vermijs, A.Solignac *et al.*, *Nature Communication* 7, 10854 (2016).
14. Y.-C.Lau, D.Betto, K.Rode *et al.*, *Nature Nanotechnology* **11**, 758 (2016).
15. Y.-W.Oh, S.-H. Chris Baek, Y.M.Kim *et al.*, *Nature Nanotechnology* **11**, 878 (2016).
16. C.K.Safeer, E.Jué, A.Lopez *et al.*, *Nature Nanotechn*ology **11**, 143 (2016).
17. A. Makarov, T. Windbacher, V. Sverdlov, and S. Selberherr, *Semiconductor Science and Technology* **31**, 113006 (2016).
18. T.Gilbert, *IEEE Transactions on Magnetics* **40**, 3443 (2004).
19. A.D.Kent, B.Ozylimaz, and E.del Barco, *Appl.Phys.Lett*. **84**, 3897 (2004).
20. G.Finocchio, M.Carpentieri, B.Azzerboni *et al.*, *J.Appl.Phys.* **99**, 08G522 (2006).